CYCLONE TESTING STATION

SCHOOL of ENGINEERING and PHYSICAL SCIENCES

James Cook University

Response of Metal Cladding Systems to Windborne Debris Impact

Report: TR59
November, 2012

Cyclone Testing Station
School of Engineering and Physical Sciences
James Cook University
Queensland 4811, Australia

www.jcu.edu.au/cts

CYCLONE TESTING STATION

SCHOOL of ENGINEERING and PHYSICAL SCIENCES

JAMES COOK UNIVERSITY

TECHNICAL REPORT NO. 59

Pre-Publication Version 30 Oct 2012

Response of Metal Cladding Systems to Windborne Debris Impact

By

U. Frye, J. Ginger and C. Leitch

October 2012

Bibliography.
ISBN 978-0-9873109-0-3

ISSN 0158-8338

Series: Technical report (James Cook University, Cyclone Testing Station); 59

Notes: Bibliography

Frye, Ulrich

Response of wall cladding systems to windborne debris impact

1. Wind-borne debris impact loading 2. Research and testing 3. Reaction forces – impact testing 4. Momentum and energy – dynamic impact testing

I. Ginger, John David II. Leitch, Campbell John III. James Cook University. Cyclone Testing Station. IV. Title. (Series: Technical Report (James Cook University. Cyclone Testing Station); no. 59).

Table of Contents

1 INTRODUCTION

Impact from windborne debris during windstorms is a load that is applied to buildings, in addition to the wind load. Debris mainly impacts windward walls (including doors and windows) and the upwind slope of steep pitch roofs. Studies have shown that building envelopes constructed from fibre cement or metal sheeting, glass windows, roof tiles etc. are especially susceptible to debris impact damage. Such damage can create a dominant opening in the envelope, resulting in large internal pressures and an increased probability of more serious damage to the structure.

2 WINDBORNE DEBRIS DAMAGE IN WINDSTORMS

Post windstorm damage studies have shown that damage to building envelopes is caused by many different types of windborne debris (i.e. missiles). Available debris can be classed as either unsecured objects (i.e. outdoor equipment) or fixed objects (i.e. parts of structures) that become loose under increasing wind speed. Wills et al. (1998) grouped missiles into three characteristic types; compact, rod and sheet objects, and derived conditions required for their flight. Lin et al. (2007) studied the trajectories of compact and rod-type objects both experimentally and numerically to derive empirical expressions to approximate the flight speed of those debris types as a function of travel distance and time. Holmes (2007) estimated the time taken and the distance travelled by a range of potential missiles to reach a specified speed.

The performance of building envelope systems in cyclone regions of Australia are qualitatively assessed according to the wind load standard AS/NZS1170.2 (Standards Australia, 2011) which requires the envelope component to withstand a piece of 100 mm × 50 mm timber weighing 4 kg and a steel sphere of 8 mm diameter and 2 grams mass, impacting at velocities which are a fraction of the regional design wind speeds. This test is optional with one of the aims being to circumvent the requirement of designing buildings to full internal pressure loading. If all building envelope components can be shown to resist this impact loading, the internal pressure requirement can be relaxed. The second objective is the protection of building occupants, such as in a designated shelter room.

Public cyclone shelters in Queensland require more severe testing criteria as their primary purpose is to protect the life of the occupants. Also, the debris impact loading is not optional for those buildings. The relevant test criteria are prescribed in the *Design Guidelines for Queensland Public Cyclone Shelters* (Queensland Government, 2006).

While the debris impact resistance of various building envelope products have been tested qualitatively, the response of building cladding and supporting structure to windborne debris impact has not been analysed in detail.

2.1 Types of Debris and Extent of Damage

Types of windborne debris in windstorms can range from loose objects such as unsecured equipment (e.g. outdoor furniture), tree branches, coconuts and other plant material to building components that become dislodged due to wind loading or as a result of being impacted by other debris.

Observations after past windstorm events have shown impact damage to buildings caused by structural members such as timber or steel rafters, battens and studs but also sections of roof

that dislodged from adjacent buildings. Often a "domino" effect was evident where debris from a building impacts another building downwind which in turn increases internal pressure causing the structure to fail and generate more debris which becomes available to impact other buildings downwind.

These observations highlight the importance of testing building envelope components for their resistance to windborne debris impacts.

3 THEORY OF FLIGHT AND TESTING CRITERIA

The following section provides a brief overview of previous windborne debris research and the evolution of associated testing standards and regimes in Australia.

3.1 Types of Debris

In order to enable theoretical analysis of flight initiation and characteristics, debris types are classified into three principal groups (Wills, et al., 1998) according to their aerodynamic behaviour and each type is assigned characteristic dimensions:

- 3 D compact objects

  These objects are characterised as having dimensions of the same order in all three directions (length – L or diameter – D), such as cubes, spheres or similar. Figure 1 shows a diagram of typical compact objects.

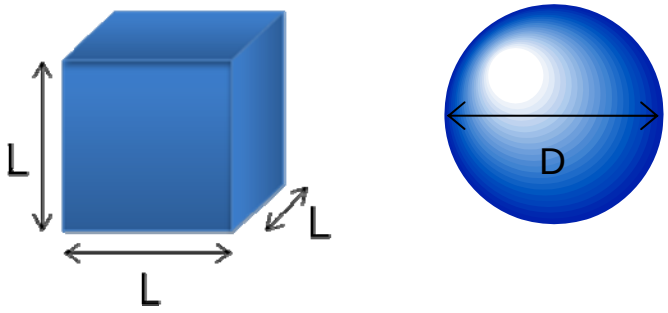

Figure 1: Compact objects showing dimensions

- 2 D sheet objects

  These objects are characterised as having dimensions of the same order in two directions (length – L and width – w) and the third dimension being much smaller (thickness – t), such as sheets of plywood, metal cladding or similar. Figure 2 shows a diagram of a typical sheet object.

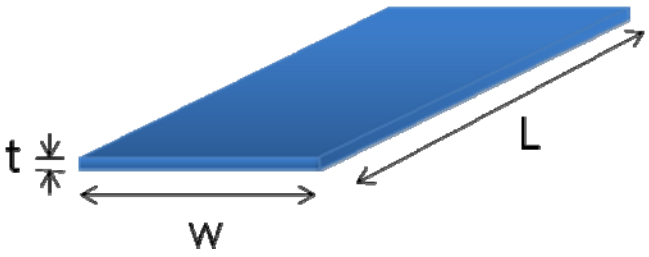

Figure 2: Sheet object showing dimensions

- 1 D rod objects

  These objects are characterised as one dominant dimension (length – L) and their cross-sectional area (A), such as sign pole, timber rafter or similar. Figure 3 shows a diagram of typical rod objects.

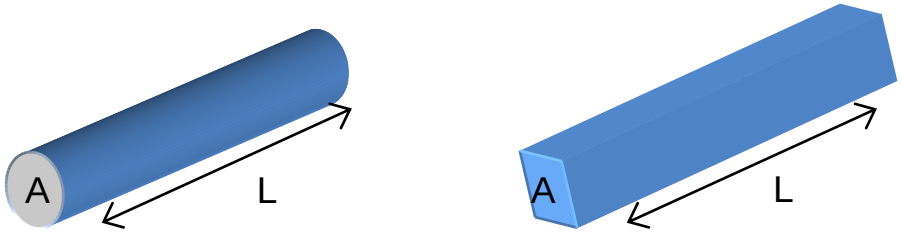

Figure 3: Rod objects showing dimensions

3.2 Debris Flight Velocities

Studies by Wills et al. (2002) and Holmes (2007) showed that the wind speed required to initiate flight of an object, U_f, is related to the density of the object and its size. Larger objects with higher density require a higher wind speed than lighter, smaller objects to attain flight. An object that is dislodged from its fixings at a wind speed higher than U_f, is able to attain a maximum velocity approaching the wind speed.

In addition to unsecured objects becoming missiles, debris from structural damage could be expected in windstorms when the gust wind speed exceeds about 50 m/s. Under such conditions, many types of potential missiles can reach speeds of 15 to 30 m/s from rest within a short space of time and distance of travel. Reitano (2003) and Ginger et al. (2004) calculated time taken and distance travelled for a range of selected objects to reach such speeds, by considering the flight patterns of compact, sheet and rod objects, and applying aerodynamic parameters, as suggested by Willis et al. (1998). Reitano (2003) determined realistic impact speeds that can be reached by these objects in a range of windstorms.

3.3 Testing Standards

The windborne debris impact test is called up in the Australian/New Zealand wind load standard AS/NZS1170.2 (2011) as an optional design load. In the Design Guidelines for Queensland Public Cyclone Shelters (2006) the windborne debris impact test is a mandatory requirement.

3.3.1 AS/NZS1170.2

This optional impact loading was first incorporated in an Australian standard in 1989. In AS1170.2-1989 it was specified that "In tropical cyclone-prone regions C and D, as defined in Clause 2.5.1, internal pressures based on dominant openings shall be used for calculating both ultimate strength and permissible stress design loads unless windows are protected against impact of debris by screens or shutters capable of resisting a 4 kg piece of timber of 100 mm x 50 mm cross-section striking them at any angle at a speed of 15.0 m/s."

The 2002 version of this standard specified in Clause 5.3.2 that "in regions C and D, internal pressure resulting from the dominant opening shall be applied, unless the building envelope (windows, doors and cladding) can be shown to be capable of resisting impact loading equivalent to a 4 kg piece of timber of 100 mm x 50 mm cross-section, projected at 15 m/s at any angle."

In the 2011 standard, the windborne debris impact criteria were amended in Clause 2.5.7 as follows: "Where windborne debris loading is specified, the debris impact shall be equivalent to -

(a) timber member of 4 kg mass with a nominal cross-section of 100 mm × 50 mm impacting end on at 0.4 V_R for horizontal trajectories and 0.1 V_R for vertical trajectories; and
(b) spherical steel ball 8 mm diameter (approximately 2 grams mass) impacting at 0.4 V_R for horizontal trajectories and 0.3 V_R for vertical trajectories."

Here, V_R is the regional wind speed given in Clause 3.2 of the standard. The following notes are also included in the clause:

1. Examples of the use of this clause would be the application of Clause 5.3.2 or the building envelope enclosing a shelter room.
2. These impact loadings should be applied independently in time and location.

The latest revision accounts for the variation in windborne debris velocities with actual wind speeds. Hence the specified impact test velocities are related to the regional design wind speed V_R, and can be anywhere between 2.4 m/s and 44 m/s. Furthermore, the ambiguity of resisting impact of the timber missile "at any angle" has been removed and is now specified to be "end on". A study by Richards et al. (2009) confirmed that this is indeed the impact orientation exerting the highest forces on the component being impacted.

Although these test criteria are optional for cyclonic regions C and D, they could equally be applied to non-cyclonic region designs, where findings of windborne debris damage after windstorms have been documented in the past, the most recent being the storms in November 2008 in Brisbane (Leitch et al., 2009).

3.3.2 Design Guidelines for Queensland Public Cyclone Shelters

Unlike the buildings discussed in the previous section, the primary objective of public cyclone shelters is to protect the life of its occupants. They are a place for people to go in the event of a cyclone and hence their design criteria are more stringent than those for ordinary buildings. The windborne debris impact criteria prescribed here are also based on regional wind speeds. Clause 3.2 of the 2006 version of the design guidelines requires that "the external fabric of public cyclone shelters to be at least capable of resisting wind debris defined as:

a) Five spherical steel balls of 2 grams mass (8 mm diameter) impacting at 0.4 $V_{10,000}$ for horizontal trajectories and 0.3 $V_{10,000}$ for vertical trajectories (Test Load B);

b) A 100 mm x 50 mm piece of timber of 4 kg mass impacting end-on at 0.4 $V_{10,000}$ for horizontal trajectories and 0.1 $V_{10,000}$ for vertical trajectories (Test Load A).

Appendix 1 of the design guidelines specifies the acceptance criteria for the external fabric as follows. For a test specimen to pass the test, it shall:

a) Prevent a debris missile from penetrating;
b) If perforated, have a maximum perforation width of less than 8 mm;
c) In the case of a debris screen, not deflect more than 0.8 times the clear distance between the screen and the glazing, at any stage of the test.

4 THE BUILDING ENVELOPE

The building envelope is generally defined as any part of the building that is exposed to the outside and protects the inside (i.e. walls and roof). Items that are integral with either walls or roofs, such as doors, windows, skylights, etc. are also considered part of the envelope. In addition, there may be other components installed on the outside of the envelope such as shutters or screens; these components may fulfil varying roles, ranging from sunlight protection, keeping insects outside or protecting windows from windborne debris impact.

All building envelope components and those installed outside of it are potentially subject to windborne debris impact. Windward walls are most prone to debris impact, because of their proximity to the ground and their vertical orientation which would interfere with objects travelling horizontally. Roofs are less likely to be impacted by windborne debris due to their distance from the ground and their inclination. In the event that a roof is being impacted, the striking object would most likely originate from above the roof, for example a dislodged item from a higher neighbouring building, a tree branch or similar. For those impacts, the debris' trajectory would almost certainly not be horizontal due to gravity acting on the object. Leeward and side walls are subjected to suction pressures and are also unlikely to be hit by debris.

4.1 Walls

Currently there are many different methods of constructing walls in buildings. For residential housing, the most common types are frames (either timber or steel) with some external cladding and an internal lining or masonry (block or brick) construction. Commercial and public buildings also employ those construction techniques but other options include portal frames with girts and external cladding, pre-cast tilt up concrete panels or concrete walls poured in situ.

4.1.1 Masonry

Masonry walls are built from masonry units on a mortar bed. There are two principal types of masonry units, blocks and bricks. Blocks are usually large hollow units and bricks are smaller in size and either solid or have small cores. The most common *nominal* size of blocks is 400 mm long, 200 mm wide and 200 mm high; however, their *actual* dimensions are 390 mm long, 190 mm wide and 190 mm high. The difference between nominal and actual size is due to the allowance for 10 mm wide mortar joints. Blocks with 200 mm nominal width are referred to as the 200 mm series. Other, less common widths are the 100, 120, 150 and 300 mm series. For simplicity of construction, ¼, ½ and ¾ blocks are also used. Bricks are usually made to traditional size, 230 mm long, 110 mm wide and 76 mm high (Concrete

Masonry Association of Australia, 2007). Figure 4 presents diagrams and photographs of a typical block and a brick.

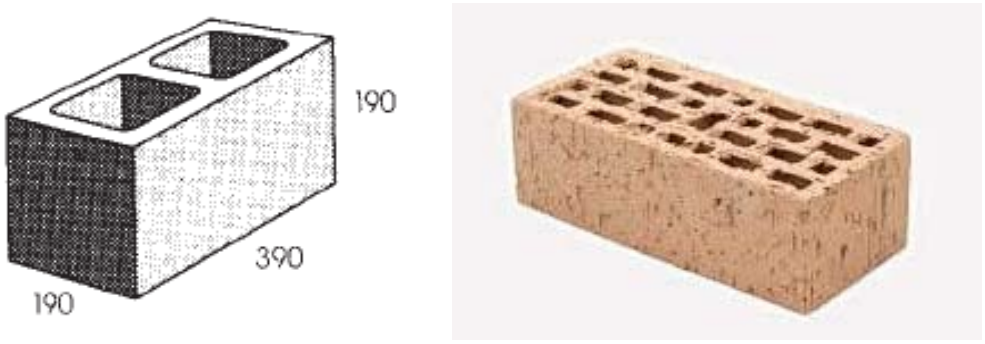

Figure 4: Typical hollow block (left) and hollow brick (right)

Single-leaf wall systems are used in the majority of cases for block wall construction. The cores of masonry block units are filled with grout (workable concrete) and reinforced with horizontal and vertical steel bars. The level of core filling (i.e. at specified cavity spacings) and size of steel bar reinforcement is usually dependent on the strength requirement of the building in question with regards to dead, live, wind, snow and earthquake loading.

Brick walls can be constructed either as single-leaf or double-leaf cavity systems. Ties, connectors, reinforcements in form of bars or wire mesh are used in combination with grouting to meet strength requirements for dead, live, wind snow and earthquake loading.

For practical purposes, masonry block walls are generally deemed to resist windborne debris impacts and are not usually tested. Due to their sturdiness and perceived strength it is widely accepted that they would withstand the standard impact test loads.

Brick veneer is another masonry construction method primarily for residential housing. Either steel or timber framing is lined internally with gyprock boards or similar. The outer face of the building consists of bricks; this outer brick layer is not considered to provide any structural support and is considered a form of external wall cladding.

4.1.2 Concrete

Concrete construction is primarily used for commercial and industrial buildings but also in high rise office and apartment buildings or public institutions. These walls are usually erected using tilt-up concrete panels. The panels are pre-cast to the required size and incorporate a steel mesh for added tensile strength. Common thicknesses range between 100 mm and 200 mm but there are virtually no limits to the size and thickness of pre-cast concrete panels. Concrete panels can be used either as cladding in a portal frame construction or form part of the load-bearing structure of a building. Figure 5 shows a concrete tilt-up wall under construction and a finished concrete building.

Figure 5: Concrete tilt-up buildings during and after construction

4.1.3 Metal Cladding

Metal wall cladding is most commonly installed on buildings such as sheds, warehouses and commercial low rise structures, but also, to a lesser extent on residential housing. Metal wall cladding is available in a wide variety of materials, profiles and thicknesses. The most common types are made from flat steel coils which are roll formed into a profile for increased strength (stiffness) and aesthetics. Other metals for wall cladding include aluminium, copper and zinc, where the manufacturing process is identical to that of steel cladding. Figure 6 shows examples of installed metal wall cladding on industrial and residential buildings.

Figure 6: Metal wall clad buildings

The wall cladding is connected to the wall girts either pierce fixed using screws or “secret fixed” by some clipping system (in some cases in combination with screws) pertaining to a particular product. Typical screw fixed cladding profiles can be grouped into three general categories: corrugated, trapezoidal rib/pan and square rib profiles. Examples of these profiles are shown in Figure 7.

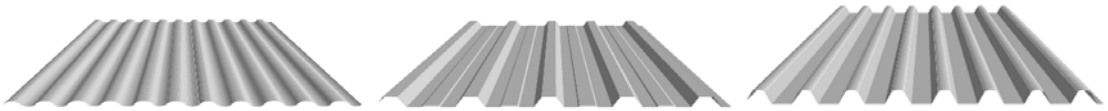

Figure 7: Typical corrugated (left), trapezoidal rib/pan (centre) and square rib (right) profiles

The grouping of "secret fixed" wall cladding is somewhat more difficult as a vast variety of options exist. They range from low profiles resembling wall boards to flat sheets with upstanding, flat or recessed seams. A few examples are shown in Figure 8.

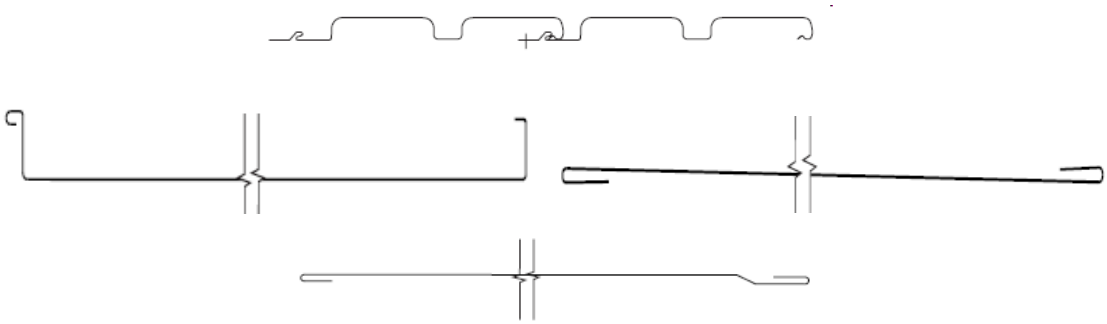

Figure 8: Profiles of typical wall board (top left) and flat sheets with upstanding (top right), flat (bottom left) and recessed (bottom right) seams

4.1.4 Fibre Cement Cladding

Fibre cement cladding is most commonly installed on residential housing. It is available in different thicknesses as flat sheets or profiled for visual appearance. This type of cladding, similar to metal cladding, is typically screw or nail fixed to the building's timber or steel frame. Fixing options include face fixing or concealed fixing, depending on the product.

4.1.5 Weatherboards

Weatherboards, like fibre cement cladding, is predominantly installed on residential housing. It is typically made from hardwood planks, although in recent times reconstituted hardwood is being used for the majority of products. The methods of installation are also identical to fibre cement cladding where the boards are directly screw or nail fixed to the steel or timber frame of the building. Weatherboards are produced in plank form and are either lapped or joined by manufactured grooves.

4.1.6 Composite Panels

Composite wall panels typically consist of two outer skins bonded to an inner core. The skins are usually made from metal, fibre cement or weatherboards and the core is some insulating material such as expanded polystyrene or mineral (fibreglass) wool. These composite panels are most commonly selected for their insulating properties and can be supplied with either flat or profiled sheets for varying appearance.

4.2 Windows

Glass windows are found on all types of buildings, ranging in size from 0.01 m^2 in toilet rooms to entire facades of high rise buildings and therefore can be parts of the building envelope or almost constitute a building envelope in itself. Consequently, there is a wide range of requirements that must be met by glazing for different applications.

While small windows in residential housing may only provide an opening for daylight and ventilation purposes, large glazing panels in commercial buildings are required to provide wind load resistance, UV light protection, thermal insulation, resistance to human impact, intruder resistance for shop fronts or even blast resistance for high security facilities.

To achieve the manifold requirements, glass windows are available from the most basic thin, single layer panels over tempered and toughened versions up to multi-layered laminated products.

4.3 Doors

External building doors serve two main purposes, providing human access and access for vehicles and goods. Depending on the purpose, doors vary in size between 0.8 m x 2.0 m for a standard personal access door up to (and possibly exceeding) 15 m x 15 m for large access doors enabling trucks to enter warehouses or similar. Special applications would include even bigger openings, such as for airplane hangars.

4.3.1 Personal Access Doors

This type of door is found on all types of buildings, allowing occupants to enter and leave. It is typically hinge-mounted along a vertical edge, although sliding configurations are also used. For residential buildings, the most basic external door is of dimensions 820 mm x 2040 mm x 35 mm and made from blockboard with plywood facing.

There is no limit to the variations for personal access doors. These range from simple incorporation of viewing panels or frosted glass for aesthetic purposes to wider openings (required in public buildings, e.g. for wheelchair access). Also, different manufacturing methods using different materials such as solid ply laminated doors are available. For added strength or security, doors can be clad with steel sheets (either external only or both faces).

Commercial buildings often have metal (aluminium) doors with proportions of glass between 20% and 80% for a more open feel to clientele and customers.

4.3.2 Vehicles and Goods Access Doors

Vehicles and/or bulky items entering buildings require larger access openings, which in turn need to be closed when not in use. Available types of doors for these applications are rolling curtain doors, roller shutters, sectional overhead doors, rigid (tilting) overhead doors, hinge-mounted doors, folding doors and sliding doors.

4.4 Screens

Several types of screens can be installed in front of windows and doors for varying purposes. Most basic flyscreens, which are a woven mesh made from fibre glass, nylon or other polyester, only serve the purpose of keeping insects outside of buildings. These are often

combined with a large aperture lockable metal grille with security in mind which allows occupants to leave windows open. Stronger woven wire mesh or perforated sheet products made from stainless or galvanised steel are also available which combine security and insect protection at the same time. Other specialised products include impact protection systems which serve the sole purpose of protecting the glazing behind from being broken by windborne objects.

4.5 Shutters

External shutters are additional components mounted in front of windows with the primary objective of providing shading and/or privacy inside but these can also offer increased security. Types of shutters include roller shutters which are integral with the window frame, fixed or adjustable louvre shutters that are either mounted within the window opening or offset outwards and overlapping, hinged or sliding shutters. Louvre shutters are also frequently installed as part of the wall, i.e. without any glazing behind. Depending on the purpose, shutters are available in various materials such as timber, aluminium, steel, plastics, etc. Shutters can also act as impact protection devices if adequately designed and tested.

4.6 Roofs

In Australia, the two most common roofing materials are tiles and metal cladding, with composite panels also being increasingly used for their insulating properties and spanning capacity. Tiled roofs are rarely found on industrial and commercial buildings. However, roof tiles are often installed on residential houses for aesthetic reasons. Metal roofing is used commonly on residential, commercial and industrial buildings.

4.6.1 Metal Cladding

Metal roof cladding is virtually identical in design and construction methods to metal wall cladding as described in Section 4.1.3. However, a few additional profiles are available that are deemed suitable by the manufacturers for roofing applications but not for walling. Roof cladding is typically crest fixed to the supporting purlins (or battens), unlike wall cladding which is usually valley fixed to the girts (or studs).

4.6.2 Tiles

Roofing tiles are available in a variety of materials and shapes. Materials include mainly concrete and terracotta (i.e. clay) but also, to a lesser extent, metal and fibre glass.

4.6.3 Composite Panels

Composite roof panels, like composite wall panels, are made from two outer skins and an insulating core. The outer skins are made from steel sheets and the core is typically expanded polystyrene foam. The external steel skin is profiled in either corrugated or trapezoidal rib/pan shape. The internal steel face can be either profiled as well or is a flat sheet. In comparison with single skin roof cladding, composite panels have the advantage of integrated insulation for thermal benefits and also provide greater spanning capacities, reducing the number of supports required.

5 RESPONSE OF BUILDING ENVELOPE TO DEBRIS IMPACT

The response of a component of the building envelope when impacted by windborne debris depends on parameters, relating to the missile itself and the properties of the envelope component or system.

The relevant parameters of the missile are its size, mass, shape, impact velocity and orientation upon impact. The properties of the envelope are its material properties such as elastic modulus (ductile materials) or rupture modulus (brittle materials), the section properties determining the stiffness, the support conditions (i.e. distance of free span) and the location of impact.

It has been shown that the worst case scenario for a rod type missile impacting a target is in the end-on orientation because all of the missile's momentum and kinetic energy are concentrated and transferred in the (comparatively) small cross-sectional area. For compact objects such as spheres the orientation of impact does not have a great effect because, by definition, this type of debris has similar dimensions in all three planes. For sheet objects it can be inferred from the rod type analysis that an end-on impact (i.e. the thickness of the sheet being perpendicular to the target) is most critical because all of the sheet's momentum and kinetic energy would be transferred through the very thin dimension, resulting in a shearing mechanism similar to a cutting action (chopping).

5.1 Qualitative Testing

Windborne debris impact testing to both AS/NZS1170.2 (Standards Australia, 2011) and the Public Cyclone Shelter Design Guidelines (Queensland Government, 2006) are both qualitative as the assessment provides only a pass/fail outcome and quantitative measurements are not made. The only exclusion is the case of debris screens that are intended to be mounted as glazing protection, which requires a maximum deflection less than the clear distance between screen and glass, and the screen deflection has to be measured while the test specimen is subjected to the impact loading.

Although the component's resistance to windborne debris impact is assessed, actual applied forces or reactions are not measured, making it almost impossible to confidently infer or predict the likely response of another similar item. In addition, analytical solution techniques are not available, so every single product has to undergo verification and certification by test, which in turn is costly for manufacturers.

However, qualitative assessment after impact testing can still provide valuable insight into a component's behaviour such as observation of the failure mechanism or the extent of damage and deformation.

A range of building envelope components and systems have been subjected to both types of impact test loads (timber rod and steel spheres) at varying impact velocities and locations. Whilst the small steel sphere impacts have only a very small damage potential to most products, the impact of the 4 kg piece of timber has been observed to create severe damage in some cases. Further, these qualitative tests allow the determination of the most critical impact locations for typical envelope components and systems.

5.2 Quantitative Testing – Metal Cladding

The Cyclone Testing Station conducted a study to investigate the quantitative response of a typical wall cladding system to impact loads. This study is aimed at identifying the

mechanisms of force transfer and load dissipation during impact loading. As the first step, generic corrugated wall cladding was assessed when subjected to both static and impact loading.

For the impact tests, two timber missiles of different mass but identical cross-sectional areas were used. Proposed parameters to be measured included the actual force that the missiles exerted on the cladding and also the reaction force that is experienced by the supporting structure. While it is in theory possible to measure the force applied by the missile by either direct use of a load cell or integration of accelerometers into the missile, this option was discarded due to difficulties sourcing adequate equipment (at reasonable cost). Thus, only the reaction forces transferred from the wall framing girts to the supporting structure were recorded by means of a high frequency response force sensor.

Two series of static tests were undertaken; the first series involved loading of the cladding specimens at constant load at various locations with the aim of determining the cladding's basic behaviour and to derive influence coefficients for the support reactions and cladding deflections. The applied load, load transferred to the supporting structure and deflections of the cladding test specimen were recorded. The second series of static tests involved testing to failure, i.e. the loading of the cladding was increased gradually until the cladding could not sustain the applied load any further. The static loads were applied via a timber piece of identical cross-sectional area to the missiles used for the impact test series.

5.2.1 Experimental Set-Up

The wall cladding used for all tests was 0.42 mm Base Metal Thickness (BMT) corrugated cladding manufactured from G550 steel (rolled from steel coil of minimum 550 MPa yield strength).

The cladding was screw fixed according to manufacturer's instructions to Z15015 purlins (1.5 mm BMT G450 steel) using 14-10 x 25 mm self-drilling metal screws at alternate valleys. A single span arrangement was investigated with the distance between girts being fixed at 900 mm.

The girts were supported at four corners by simulated standard cleats, spaced 1500 mm along the purlin. One of the cleats had been fabricated to accommodate a three-component piezoelectric force sensor (able to measure forces in three dimensions, i.e. x, y and z directions) with very high frequency response, which was mounted between the girt and the supporting structure.

In the early stages, two lapped sheets of cladding were used but this was changed during the course of the program to two single (not lapped) sheets.

Figure 9 shows the initial set-up using two lapped sheets, and a grid of thirty points on the specimens, identified as points A0 to E5. The spacing between these grid points (x = 300 mm, y = 225 mm) being parallel and perpendicular to the girts, respectively, and the force sensor was located at point A0.

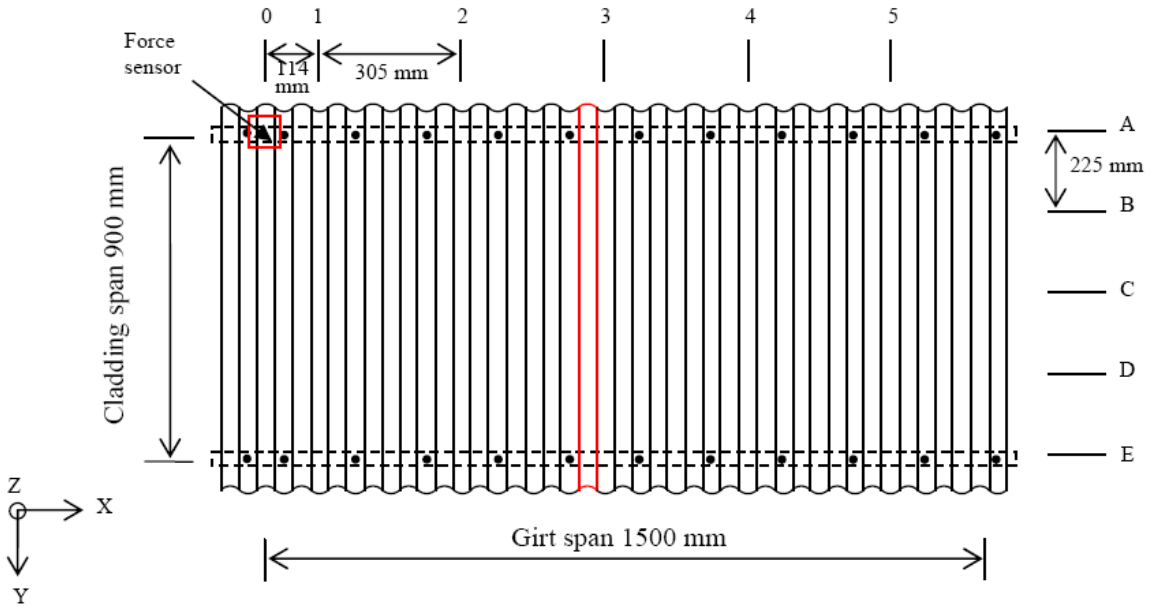

Figure 9: Diagram of initial experimental set-up

5.2.2 Static Testing

The first series of static tests was performed in the elastic region of the cladding material with the aim of investigating the fundamental behaviour of this cladding profile. A load of nominally 500 N was applied at each of the grid points via a piece of timber with a cross-sectional area of 100 x 50 mm. This load was applied with a hydraulic ram operated by a hand pump. A load cell was placed between the ram and the timber piece to monitor the load applied to the cladding. The force sensor mounted at location A0 was used to record the x, y and z directional reactions at that location, when the cladding was loaded at each grid point. This allowed the derivation of influence coefficient to determine load sharing between support points.

Two sub series of these static tests in the elastic region were performed; the first series involved force measurements only and the second series also included deflection measurements of the cladding. Digital dial gauges were positioned on the internal face of the cladding at points B1, B2, B3 and C1, C2, C3 and deflections were recorded once the nominal load was applied.

Another two static tests were undertaken, where the cladding was subjected to the same loading method as previous, without deflections being recorded. However, in these two tests

the load was increased until the cladding could not sustain any more applied force. In these cases, the cladding was either perforated or deformed to such an extent that it had failed locally. For these two tests, the reaction at the cleat interface was not recorded; the sole purpose of this series was to establish an upper bound of applied force that the cladding system can sustain.

5.2.3 Dynamic Impact Testing

Two series of impact load tests were conducted. The first series involved a small piece of timber of 0.775 kg mass and 100 x 50 mm cross-sectional area being dropped from a height of 200 mm at each of the thirty grid points on the cladding specimen. The set-up was identical to the static tests, i.e. the reactions at the cladding to structure interface were measured by the force sensor. The drop height was chosen to be low in order to maintain the cladding behaviour within the elastic region. This allowed subsequent comparison with the results obtained from the static tests in the elastic range.

The second series of impact tests was conducted with two different timber missiles. The first one being the small missile (0.775 kg, 100 x 50 mm cross-section) and the second missile being the "standard test missile", the 4 kg piece of timber having a cross-sectional area of 100 x 50 mm. The two missiles were dropped at selected grid locations (A1, B1 and C2) on the cladding specimens at various impact velocities. During the impact events, the reactions at the cladding to structure interface were recorded with the force sensor; this data acquisition was performed at a rate of 25 kHz.

6 RESULTS, ANALYSIS AND DISCUSSION

The following section provides a summary of the results, their detailed analysis and also a discussion of the findings.

6.1 Qualitative Testing

A variety of products have been qualitatively assessed to ascertain their response windborne debris impact. The tests included both Test Loads A (4 kg timber missile) and B (2 g steel spheres) at a range of impact velocities. Included in this report are the tests carried out on metal cladding wall and roof systems.

6.1.1 Metal Cladding Systems

Two 0.48 mm thick metal cladding profiles were tested to assess their impact resistance; the profiles were a corrugated profile and a square-rib profile. Both cladding products were installed in a 900 mm triple span arrangement using two sheets (to incorporate a side lap) and fixed to Z15015 purlins. The cladding was installed in roofing configuration, i.e. crest fixed to manufacturer's specifications with the use of cyclone caps for high wind applications.

The square-rib profile was subjected to the small steel spheres impact test loading at a velocity of 34 m/s and passed the test with only minor indentations in the steel material. The 4 kg timber test load was applied at a velocity of 8.5 m/s for vertical trajectories at seven different locations on the test specimen. The cladding passed all tests with the amount of damage extending to deformation/creasing only across a maximum width of two ribs.

The testing of the corrugated cladding was conducted with the aim to establish a threshold velocity at which the cladding response changes from a pass to a fail result when impacted with the 4 kg timber missile.

The corrugated cladding also passed the small steel spheres impact series at 34 m/s, showing only minor indentations after the tests.

The threshold failure impact velocity of the corrugated cladding was found to be around 25 m/s when the cladding was impacted adjacent (within 100 mm) to an internal support with the 4 kg timber missile. When the impact took place at midspan, i.e. halfway between supports, the failure threshold velocity increased to about 29 m/s. Figure 10 shows two photographs of a wall sample that had been impacted at the same velocity of about 25 m/s but at different locations.

Figure 10: Corrugated wall cladding after impact at midspan (left) and close to internal support (right) by the 4 kg timber missile at 25 m/s

It was observed that the mechanism of damage was localised for the low velocity impacts with only two or three corrugations deformed (creased). The extent of deformed corrugations increased with impact velocity up to deformation across the entire sheet (photograph on left in Figure 10). For the impacts that resulted in a failure of the cladding, the failure mechanism was an initial shear punch at the impact area followed by tearing of the cladding across the corrugations.

These observations suggest that the deformation of the cladding absorbs the missile's kinetic energy up to a threshold velocity, beyond which the material's local shear strength is exceeded, resulting in failure.

6.2 Quantitative Testing

Quantitative testing was undertaken only on the metal wall cladding system described in Section 5.2. A summary of the results are presented in the following sections along with their analysis and interpretation.

6.2.1 Static Testing – Influence Coefficients

Static loading of the cladding system was performed as described in Section 5.2.2. The response of the system to static loads is presented in terms of the x-y-z reaction at A0 (i.e. R_x, R_y and R_z). Figures 11 to 13 show the reactions R_x, R_y and R_z non-dimensionalised with the reaction R_z when the static load is applied at A0. The plotted data represent the average of two series of tests undertaken. Since the loads were applied to the cladding in the (negative) z direction, the largest reaction forces were measured in this direction, as shown in Figure 13. As shown in Figures 11 and 12, reaction forces were also present in the x-y plane of the cladding.

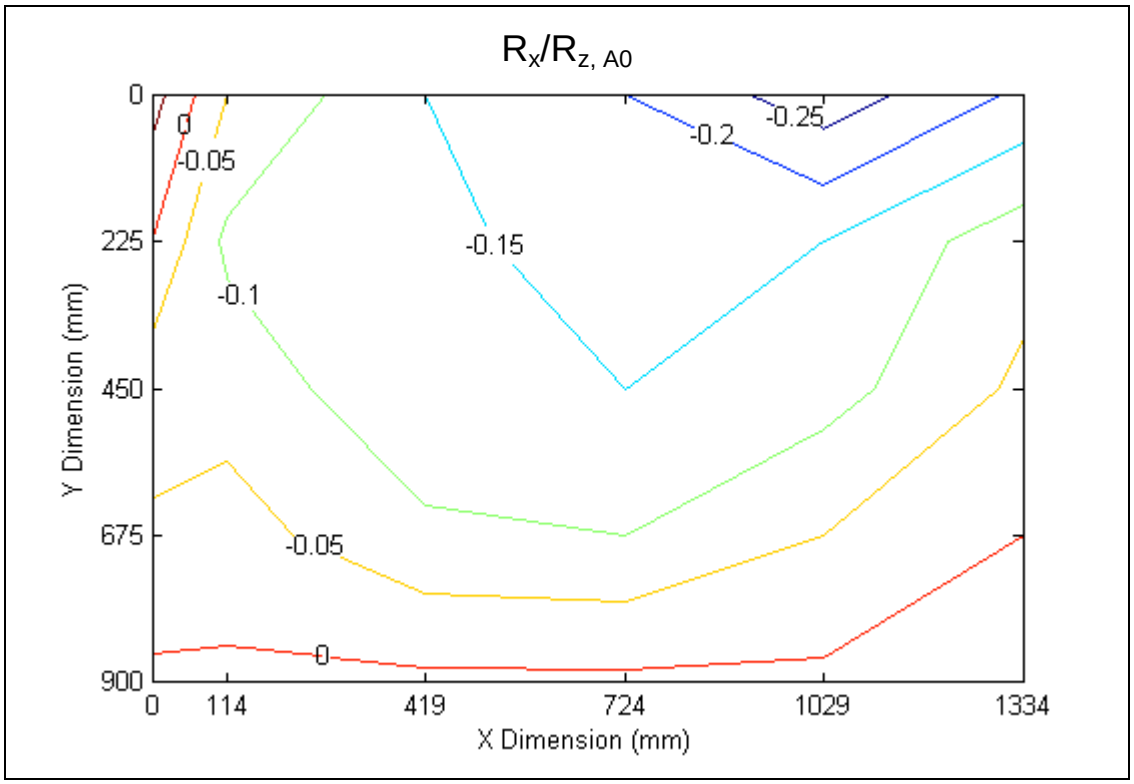

Figure 11: Influence coefficients for reactions in x direction, $R_x/R_{z,\,A0}$

Figure 11 shows that the reaction forces in the x direction, i.e. parallel to the girts, are comparatively small and only constitute a maximum magnitude of a quarter of the reaction measured in the z direction (perpendicular to the cladding) when the load is applied directly above the force sensor. It is noteworthy that all measured reactions here are negative, i.e. to the left. The likely cause of this behaviour is the spreading of the cladding corrugations, essentially pushing the fixing screws away from the point of load application (left and right). This sideways force is then transferred to the girt and ultimately to the force sensor, resulting in the measured outward acting reaction force.

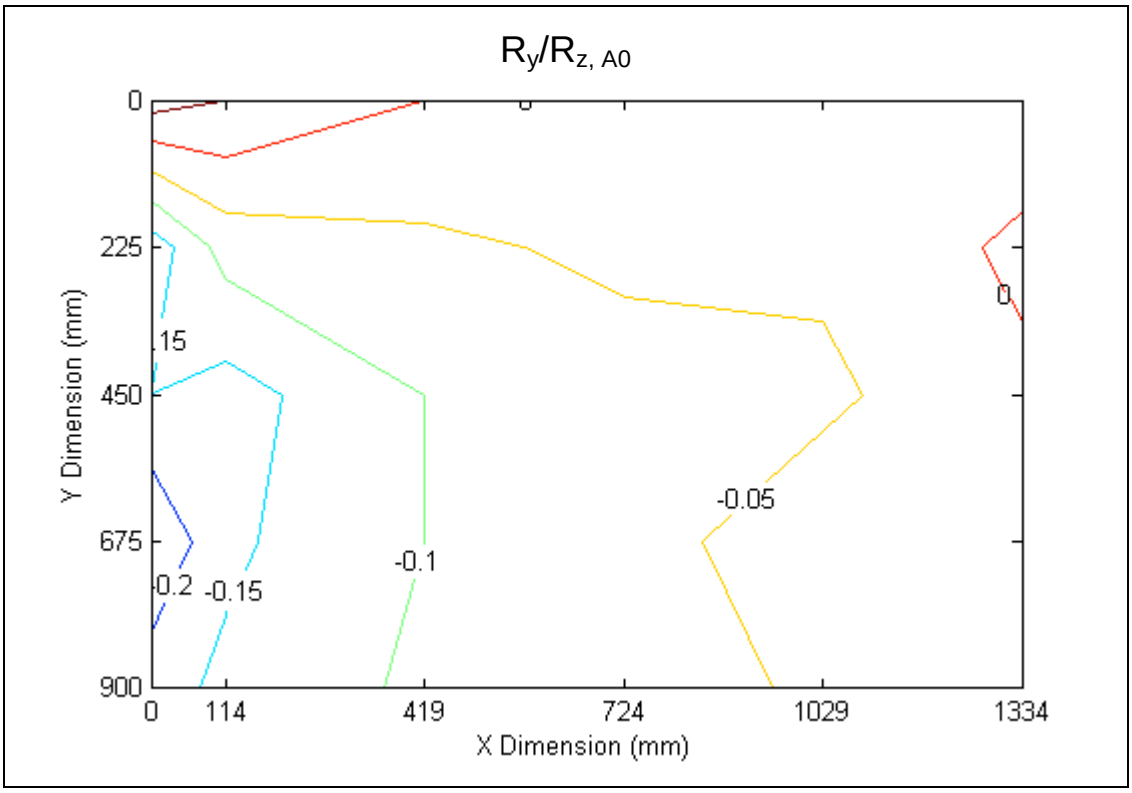

Figure 12: Influence coefficients for reactions in y direction, $R_y/R_{z,\ A0}$

Similar to the reaction forces measured in the x direction, the forces measured in the y direction, i.e. parallel to the cladding corrugations and perpendicular to the girts, are comparatively small, as shown in Figure 12. The maximum magnitude measured here was ~20% of the maximum normal force measured when the load was applied directly above the force sensor. The presence of these forces is attributed to the membrane forces in the cladding due to its deflections under load. Their magnitude increased with the distance the load was applied from the force sensor up to about the cladding midspan. Beyond the centre of the cladding span, the y reactions at A0 decreased as the higher proportion of the load was transferred to the girt on the opposite side. Somewhat unexpected here is the direction of the reaction forces; membrane force theory would suggest a tensile force being transferred from the cladding to the girts, essentially pulling the supports inwards which should result in a positive reaction force in the assigned coordinate system.

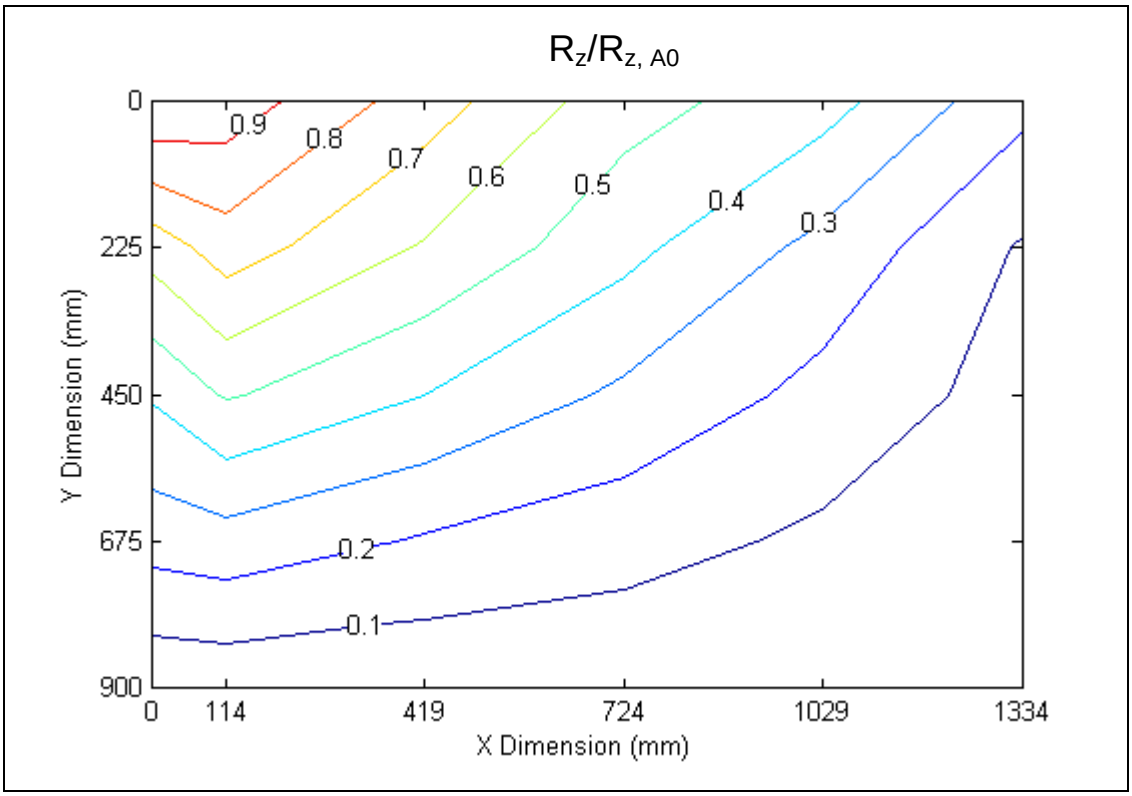

Figure 13: Influence coefficients for reactions in z direction

The plot in Figure 13 shows the influence coefficients for the reactions at A0 in the z direction, i.e. perpendicular to the cladding and parallel to the loading direction. These results are distributed as expected, with the reaction being equally shared between the two girt supports when the load was applied at midspan of the girt. Similarly, equal sharing of reaction is evident when the load was applied at midspan along the left edge of the cladding. The sharing of reactions when the load was applied at the geometric centre of the cladding specimen was expected to be in equal amounts (25%) to all four corner supports and the measured reactions agree overall.

6.2.2 Static Testing – Deflection Measurements

As part of the second series of static load tests, deflections were measured at selected locations on the cladding surface, as detailed in Section 5.2.2. The analysis of these deflection measurements provides a description of the cladding behaviour under concentrated loading in the material's elastic region. As noted earlier, six dial gauges were positioned at grid points B1, B2, B3, C1, C2 and C3. The nominal load of 500 N was then applied at each grid point A1 to E5 in turn and deflections measured at the same time as the reactions at A0. Contour plots of the measured deflections are presented in Figures 14 to 16. The actual deflections were measured in the negative z direction; however, for simplicity they are plotted as absolute numbers in the following figures.

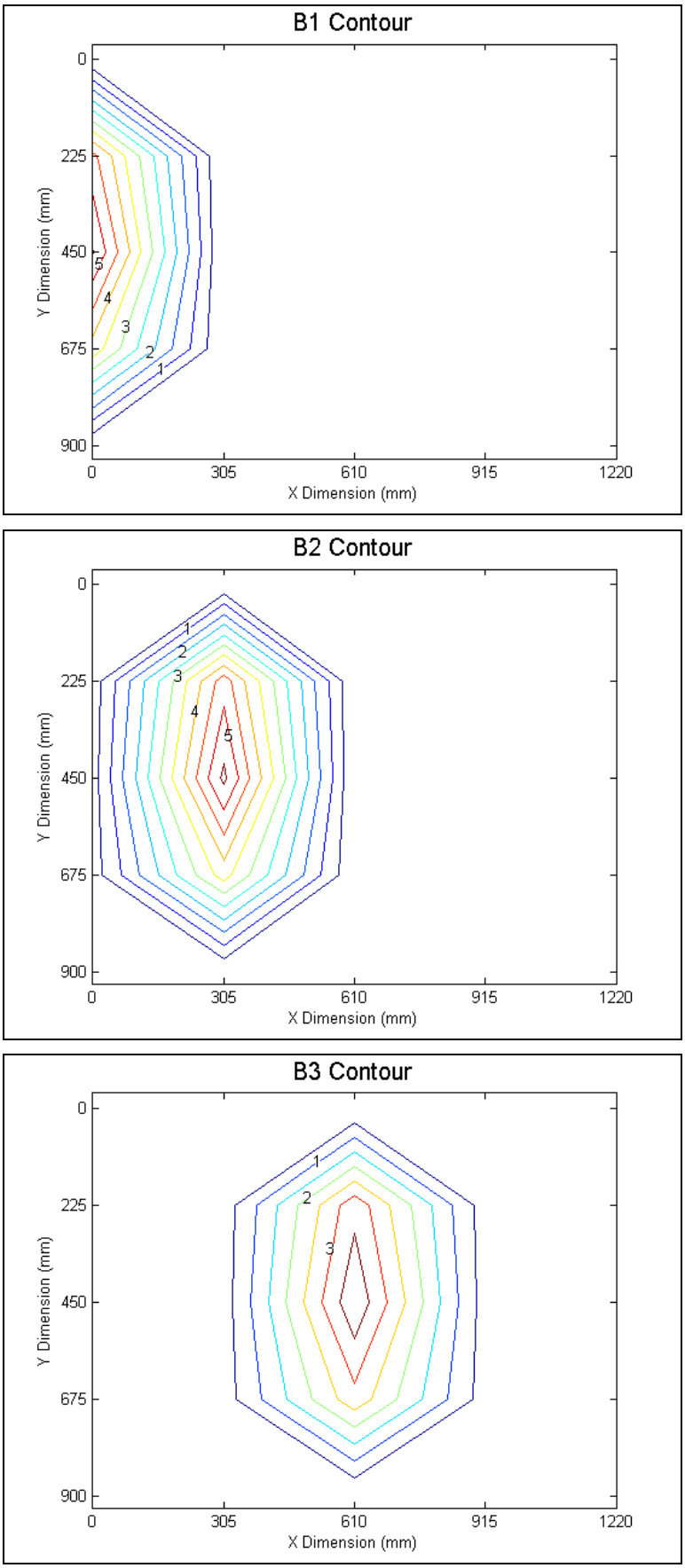

Figure 14: Cladding deflections (mm, absolute) in the z direction with loading at B1 (top), B2 (centre) and B3 (bottom)

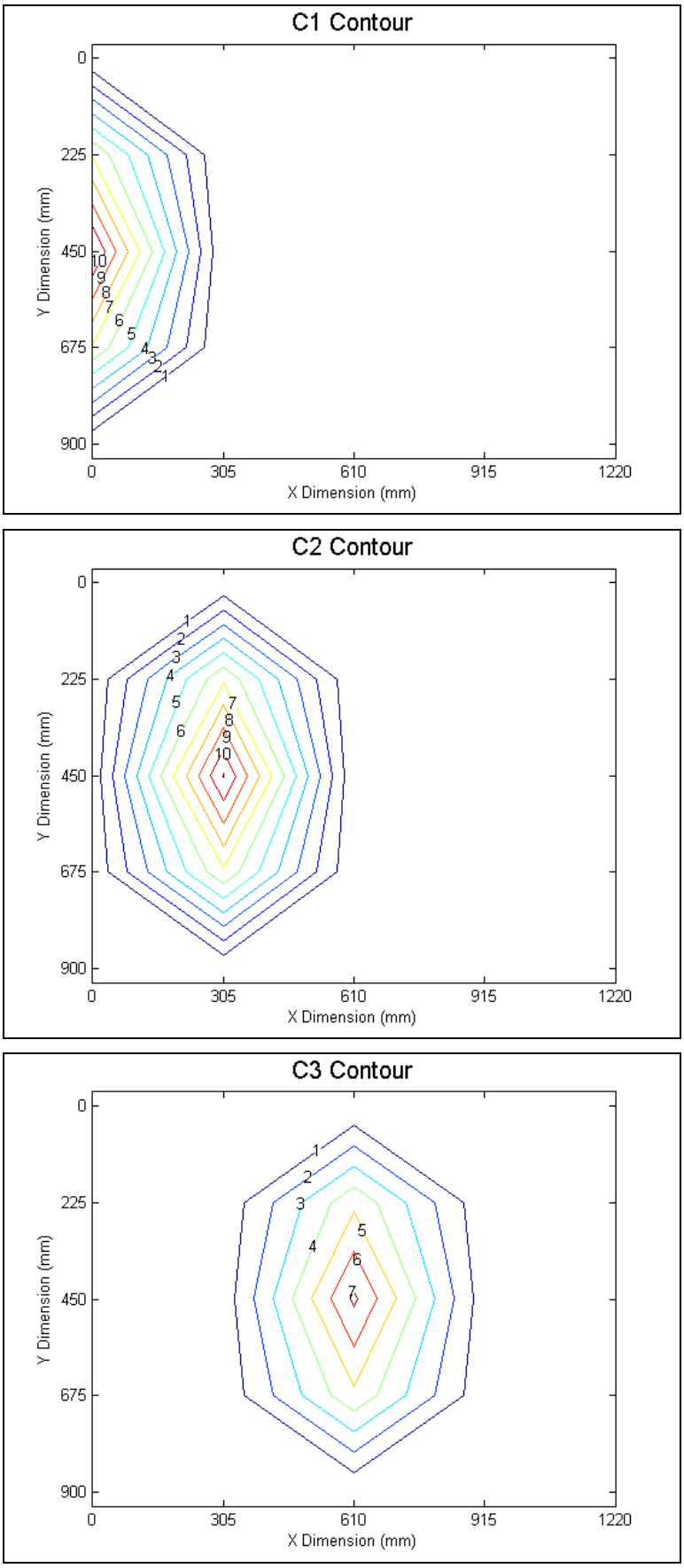

Figure 15: Cladding deflections (mm, absolute) in the z direction with loading at C1 (top), C2 (centre) and C3 (bottom)

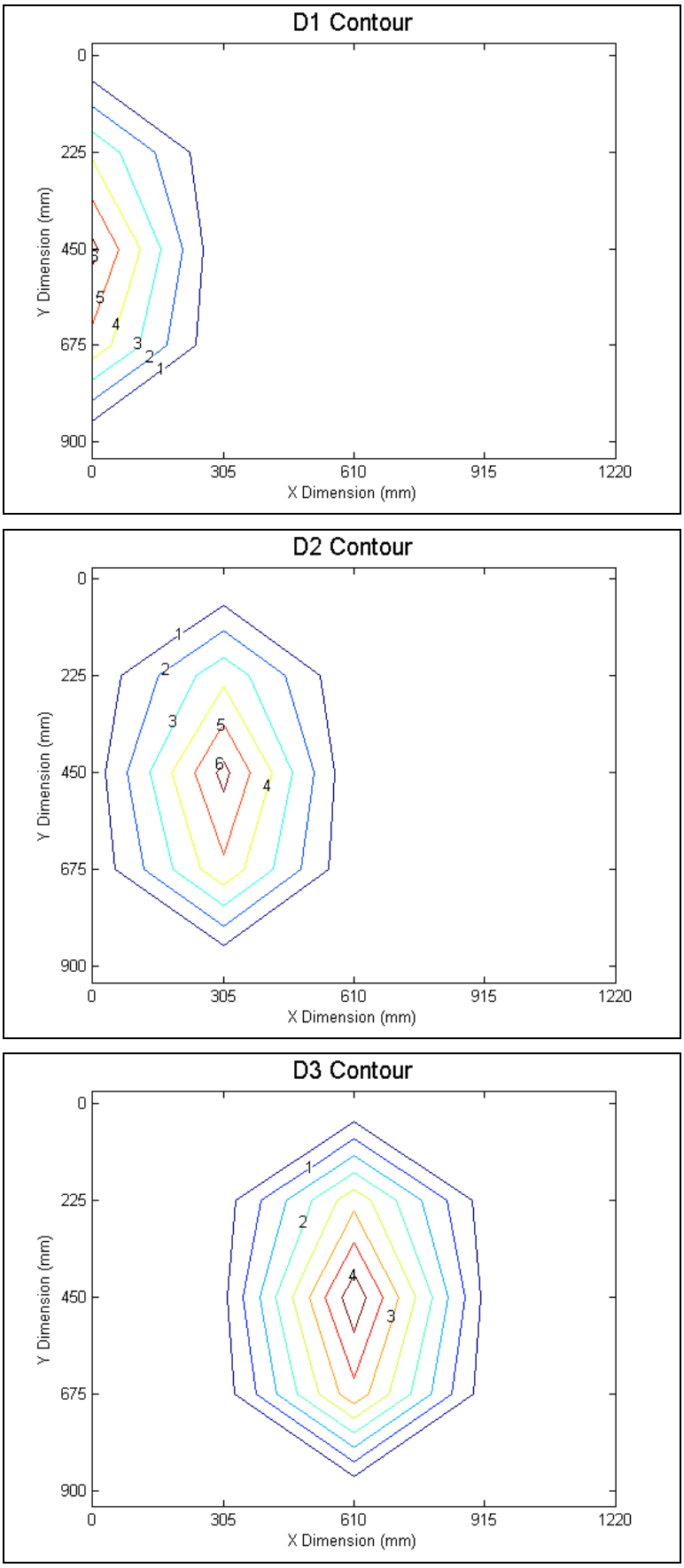

Figure 16: Cladding deflections (mm, absolute) in the z direction with loading at D1 (top), D2 (centre) and D3 (bottom)

While actual deflections were measured only at grid points B1 to B3 and C1 to C3, the assumption of symmetric behaviour (due to symmetric geometry) allows creation of the above plots, including the deflections at points D1 to D3. Loads applied at the remaining grid points A1 to A5, E1 to E5, B4, B5, C4, C5, D4 and D5 generated very small cladding deflections.

From the deflection contour plots above it is evident that the largest deflection occurs when the cladding is loaded at midspan, i.e. half way between the two supporting girts. When the specimen was loaded off centre, (i.e. lines B and D) the greatest deflections were measured at midspan (i.e. line C). The following analysis shows that this behaviour conforms to simple beam theory and the cladding essentially acts like a beam member along its corrugations. Furthermore, the measured data indicate that very little of the applied load is transferred across the corrugations, as can be seen from the rapid decay of vertical deflections in the x direction (across the corrugations).

The dial gauges were arranged on the cladding surface spaced four corrugations apart, as shown in Figure 17. When the cladding was loaded in the configuration shown, i.e. load applied in the centre of the sheet above gauge δ_2, the deflections measured at the other two gauges δ_1 and δ_3 were much smaller (less than 5 % of δ_2). Based on this, the cladding is considered to act as a three corrugation wide (229 mm) beam element in bending.

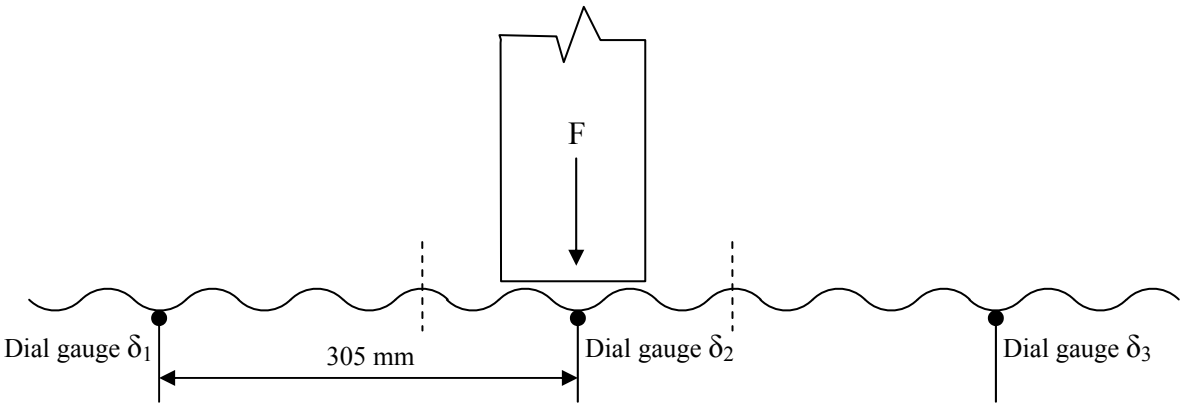

Figure 17: Schematic of dial gauge arrangement on cladding surface

The area moment of inertia (2nd moment of area) for the corrugated cross-section is I_{xx}=0.015x10^6 mm^4/m (per metre width) and the Modulus of Elasticity (Young's Modulus) of 0.42 mm BMT G550 steel was experimentally determined to be 219 GPa (Rogers & Hancock, 1997). These properties were used to compute theoretical deflection values based on a beam subjected to a point load. The calculated and measured deflection values are listed in Table 1.

Table 1: Comparison of measured and calculated deflection values

Loading Location	Deflection at B2			Deflection at C2			Deflection at D2		
	Measured (mm)	Theory (mm)	Variation (%)	Measured (mm)	Theory (mm)	Variation (%)	Measured (mm)	Theory (mm)	Variation (%)
B2	4.77	5.68	16	5.62	6.94	19	3.73*	4.42	16
C2	6.84	6.94	1	11.08	10.05	10	6.84*	6.94	1

*Values not actually measured but assumed from symmetry

The maximum variation between calculated values from beam theory and experimentally measured values is below 20 %. Considering that the cladding system is a system consisting of a number of components (cladding, fixing screws and supports) and is not a single member as assumed in the calculations, the results agree reasonably and hence the beam theory can be used to predict the response of thin corrugated cladding subjected to a concentrated load.

6.2.3 Static Testing – Ultimate Strength

Two tests were conducted on a single sheet, single span cladding specimen screw fixed to girts as previously. The first loading location was adjacent to a support (close to grid point A1) and the second loading location was the geometric centre of the sheet (grid point C2). In both cases, two corrugations were being loaded. Table 2 summarises the results and observations.

Table 2: Summary of ultimate strength test results

Loading Location	Max. Load (kN)	Observations
Close to A1	12.4	Cladding torn
C2	7.5	Cladding creased, loss of stiffness

These results provide an upper bound for the force required to induce shear failure to this particular cladding and set-up configuration. Figures 18 and 19 show photographs of the cladding specimens after the static strength tests.

Figure 18: Static strength testing near A1

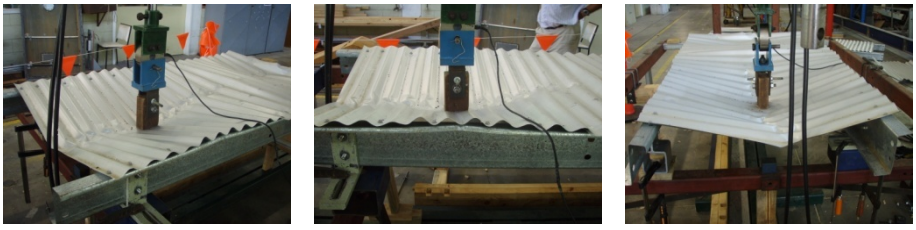

Figure 19: Static strength testing at location C2

6.2.4 Impact Testing – Elastic Cladding Response

The impact tests with the cladding response in the elastic range were conducted as described in Section 5.2.3. All 30 grid points on the cladding specimen were impacted with the 0.775 kg timber missile which was released from a height of nominally 200 mm to fall through a PVC tube incorporating a velocity meter at its exit. This drop height gives a theoretical impact

velocity of 1.98 m/s and the missiles momentum and kinetic energy of 1.53 kg.m/s and 1.52 J, respectively. However, the missile velocity measured just before impact varied and was slower by up to 20 %. For simplicity of subsequent analysis, the impact velocity for this series was assumed to be 1.70 m/s with corresponding momentum and energy of 1.32 kg.m/s and 1.12 J, respectively.

The response of the system to the low level impact loads is presented in terms of the peak x-y-z reaction at A0. Figures 20 to 22 show the peak reactions R_x, R_y and R_z non-dimensionalised with the peak R_z when the impact is at A0. Unlike the static tests, the applied load during the dynamic tests was not constant, however, as noted previously, the missile's impact velocity, momentum and kinetic energy were nominally identical for all impact loads.

Figure 20 presents the influence coefficients for the reaction at A0 in the x direction when the cladding specimen was subjected to the low level impacts. It can be seen that the x direction force contributes only a magnitude of about 15 % over an area of about 80 % of the cladding specimen. It is only along the girt incorporating the force sensor that the reaction actually exceeds the 15 % mark. Interestingly, the reaction force increases with distance away from the force sensor. This response was also observed during the static loading (see Figure 11) where the highest reaction force was measured when the load was applied at location A4; the derived influence coefficients for loading at this location are somewhat similar with magnitudes of 0.25 for static and 0.35 for impact loading. However, in the static loading case the influence coefficients in the x direction measured at A0 actually decrease to nominally zero along the girt opposite the force sensor location. In the impact loading case the lowest encountered influence coefficient is 0.15. This difference shows that the cladding system behaviour is fundamentally different for static and impact loading.

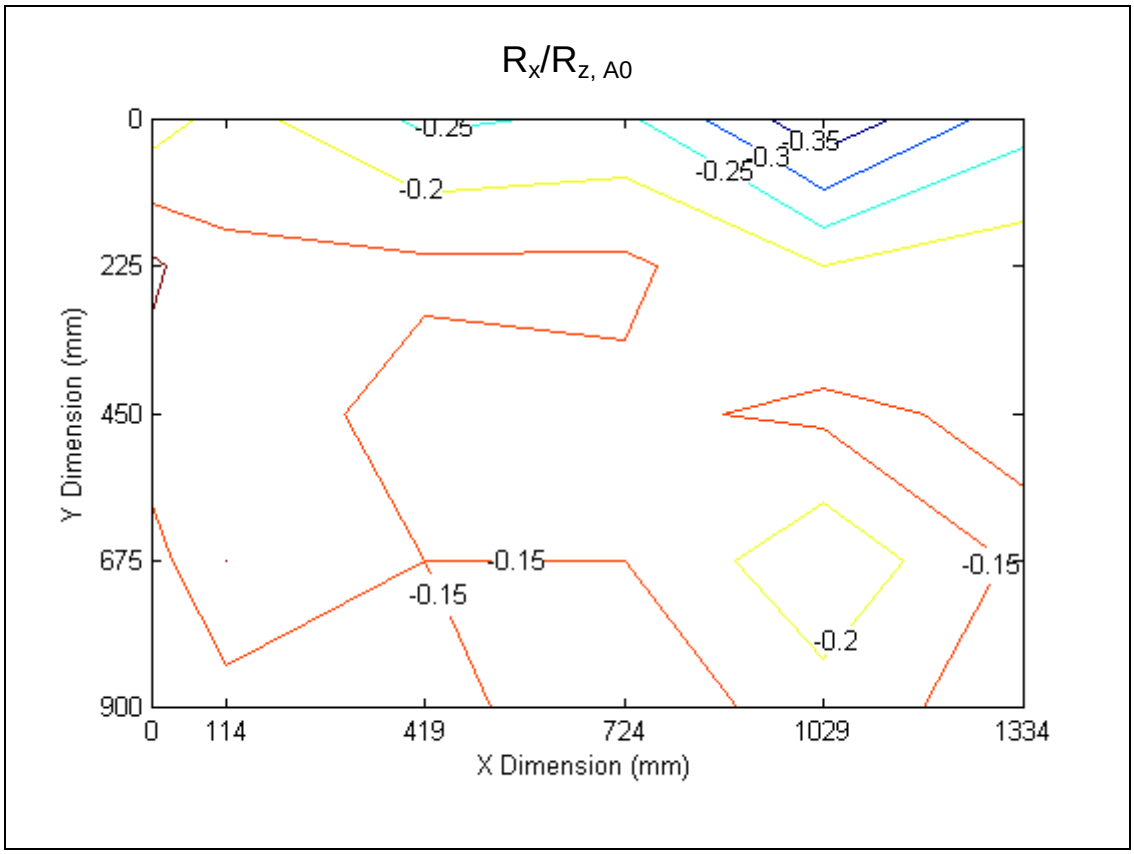

Figure 20: Influence coefficients for impact reactions in x direction, $R_x/R_{z,\,A0}$

Figure 21 is a plot of the influence coefficients for the reaction at A0 in the y direction when the cladding specimen was subjected to the low level impacts. The plot shows that the contribution of the y direction force contributes only a magnitude of about 10 % over an area of about 75 % of the cladding specimen. It only exceeds this where the impact location is close to the girt supported by the force sensor. The measured peak reaction force in the y direction was for the impact directly above the force sensor with a magnitude of 0.53 for the calculated influence coefficient.

The distribution of y direction influence coefficients is quite different compared to the static and impact loading cases. For the static loading, the influence coefficients increase only with loading along the line 0 between the two supports. This finding agrees well with the observation from the deflection measurements where the load transfer occurs mainly along the cladding corrugations.

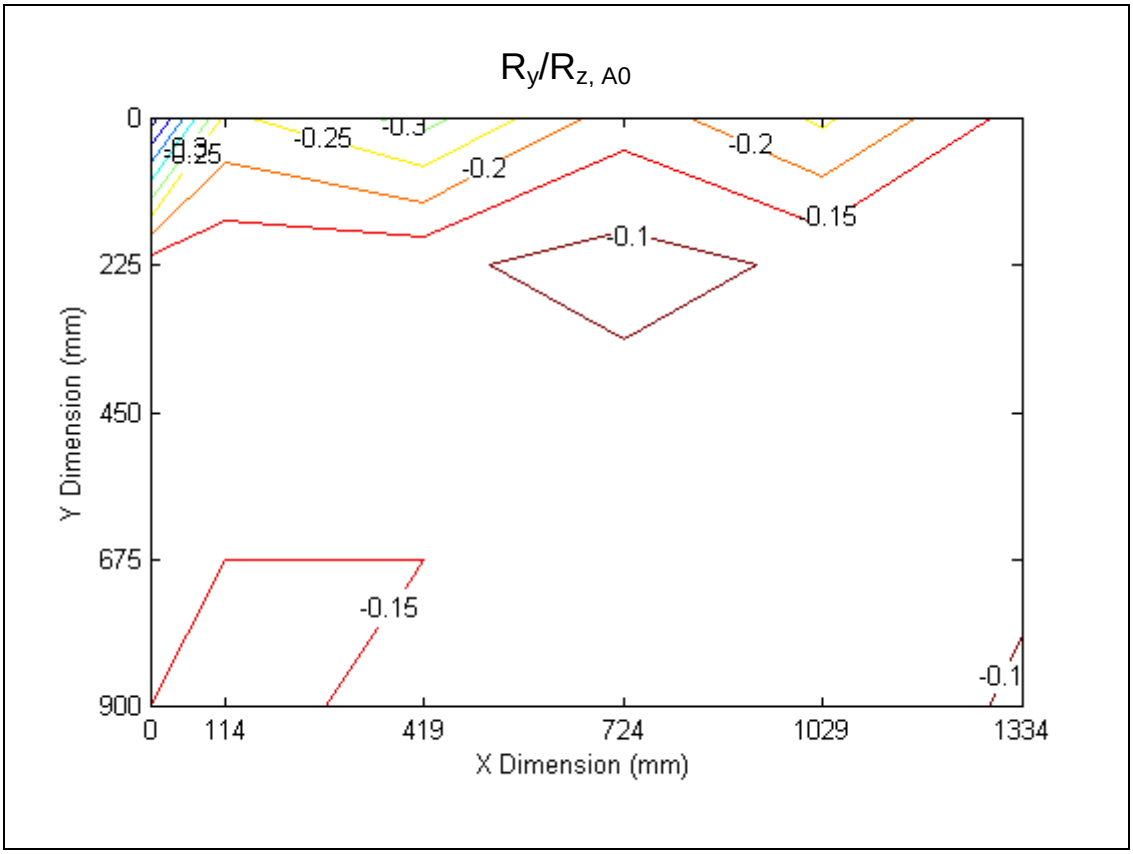

Figure 21: Influence coefficients for impact reactions in y direction, $R_y/R_{z,\ A0}$

Figure 22 is a plot of the influence coefficients for the reaction at A0 in the z direction when the cladding specimen was subjected to the low level impacts. By definition, the influence coefficient at A0 is unity; for about 85 % of the cladding specimen area the contribution of the z direction reaction force is only about 20 %. The basic shape of the influence lines for these low level impact events is comparable to those when the specimen was loaded statically. However, the decay of contribution is much more rapid and this observation indicates that the impact load itself is decreased in the free spanning area due to the cladding being able to deflect and vibrate and by these means absorb a proportion of the impact energy.

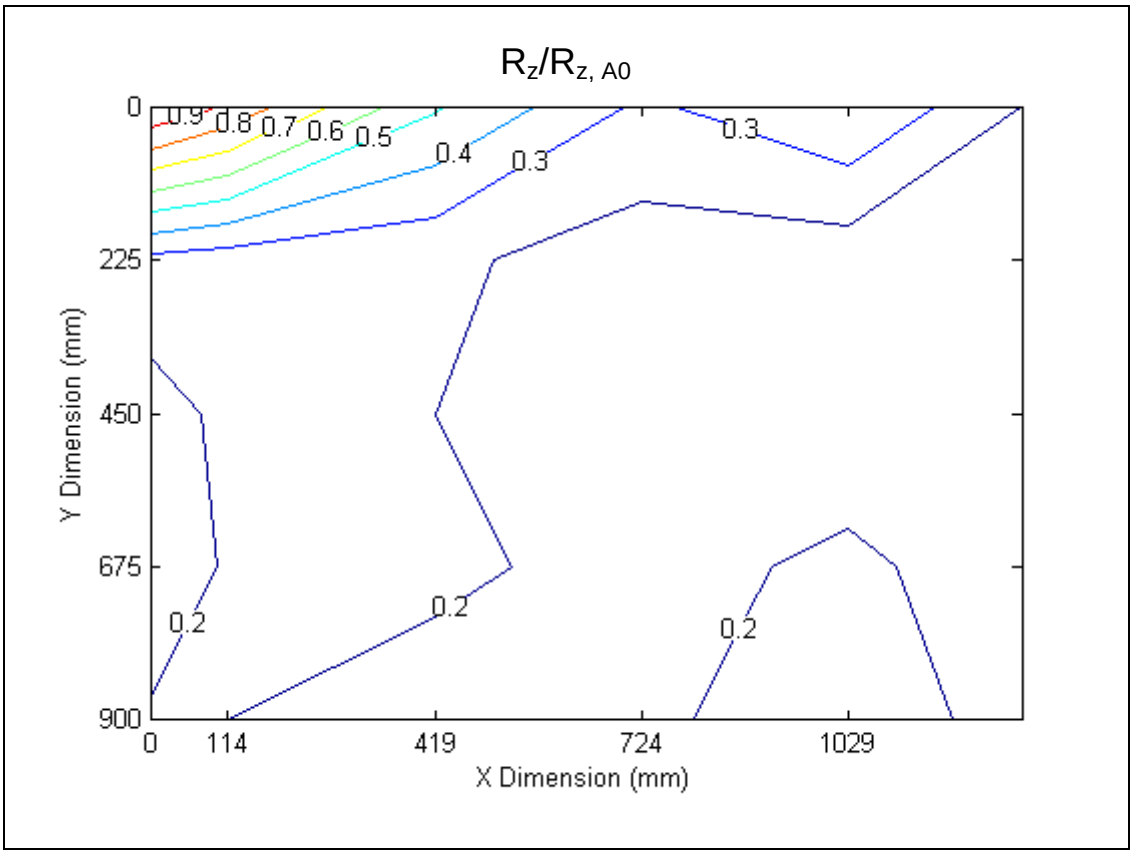

Figure 22: Influence coefficients for impact reactions in z direction, $R_z/R_{z,\ A0}$

Figures 23 to 25 show the x, y and z reaction time histories at A0 when the cladding specimen is impacted with a 0.775 kg mass at 1.7 m/s at locations A1, B1 and C2, respectively.

Figure 23 shows that the peak reaction R_z is measured within 1.9 ms of impact at A1 (above purlin), followed by a rapid drop and reversal of reaction. A similar response is also seen for R_x and R_y. Figures 24 and 25 show that the peak reactions (R_z) occurred with increasing time lags of 7.3 and 10.6 ms as the impact location moves further away to B1 and C2, respectively.

New para

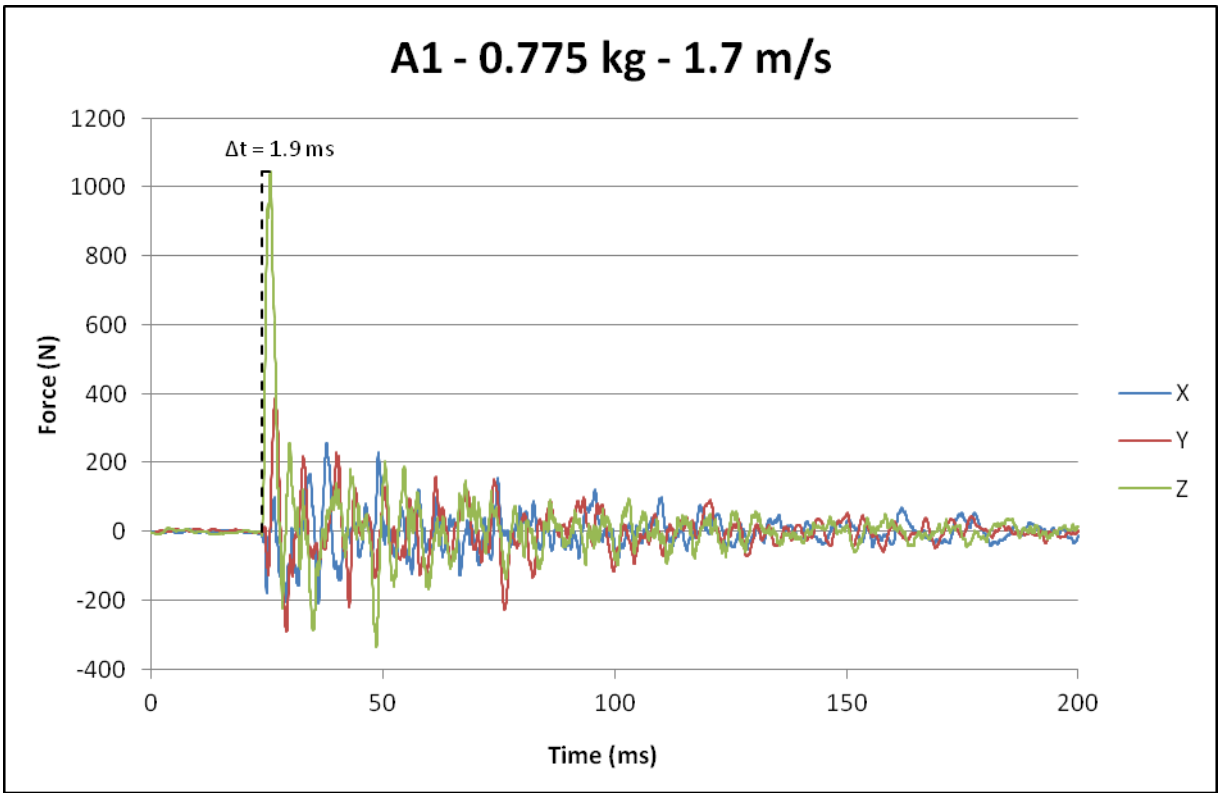

Figure 23: Time history of x, y and z reactions at A0 for impact loading at A1 by 0.775 kg timber at 1.7 m/s

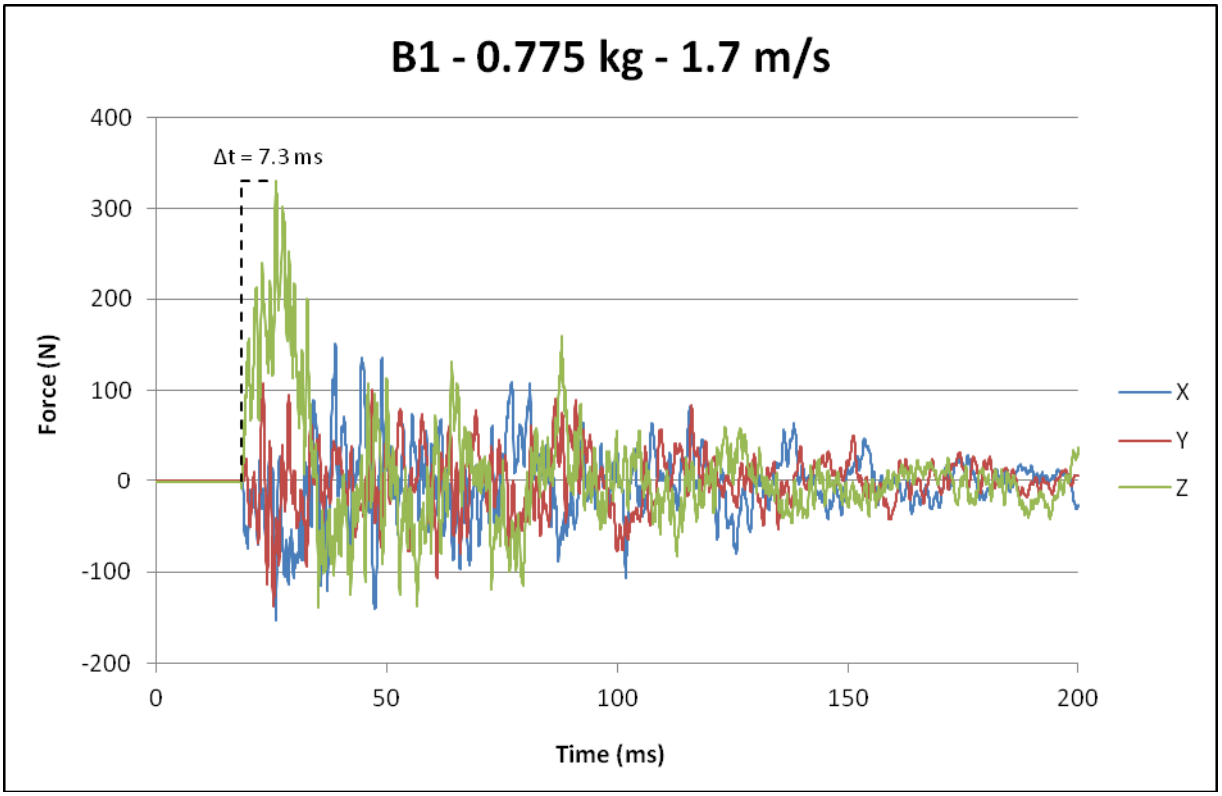

Figure 24: Time history of x, y and z reactions at A0 for impact loading at B1 by 0.775 kg timber at 1.7 m/s

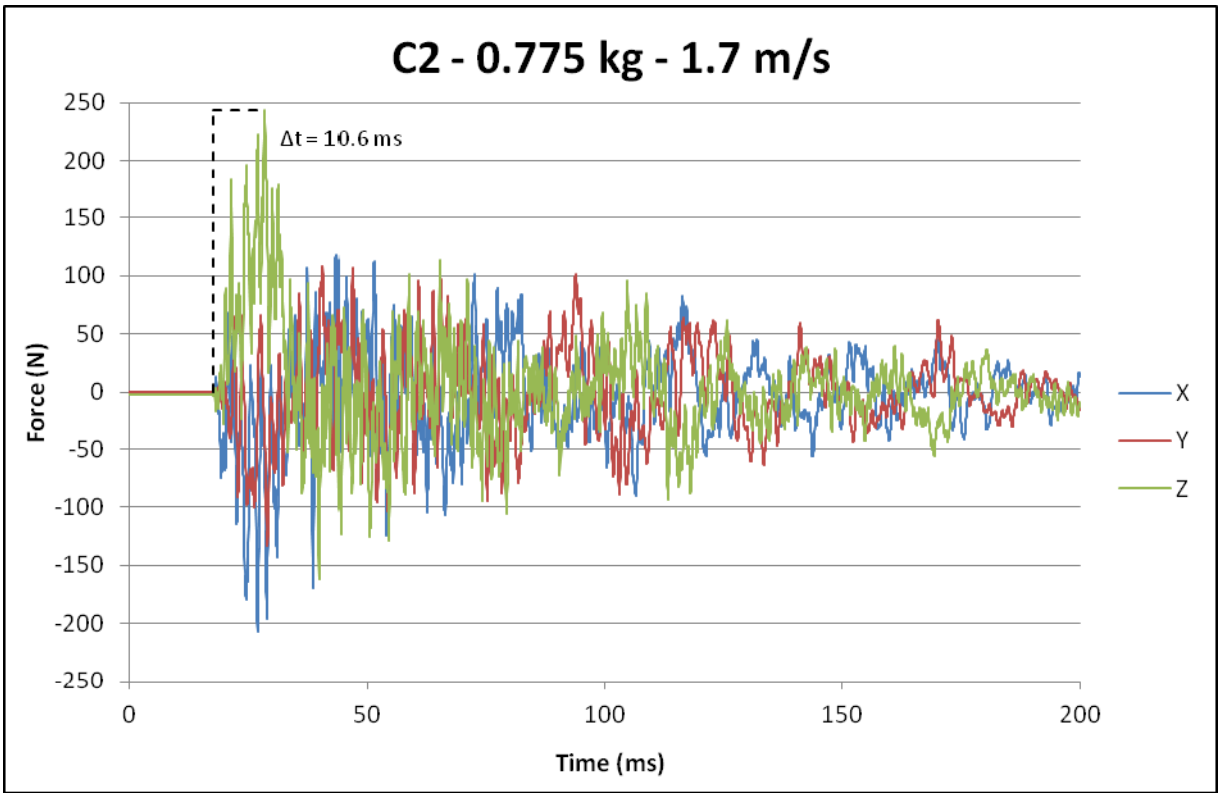

Figure 25: Time history of x, y and z reactions at A0 for impact loading at C2 by 0.775 kg timber at 1.7 m/s

A possible explanation for this trend of increasing time for the force to reach its maximum value coupled with a reduction in the value of the maximum force as the target impact point is moved from A1 to C1, relates to the reduction in relative stiffness of the different target locations. When the missile impacts Point A1, the cladding is supported by a girt directly underneath and so the stiffness of the target area is mostly controlled by the girt stiffness and the deflection will be relatively less than that for cladding only. This relatively large stiffness will also cause the maximum force generated at the target area to be larger and the time taken to reach this maximum value smaller than for the case where the missile impacts Point C2.

In contrast, the Point C2 target area is at the cladding midspan and so this point will deflect more, controlled by the much smaller cladding stiffness. For this case, it would be expected that it would take more time for this increased deflection to occur, accompanied by a relatively smaller impact force and this agrees with the experimental results.

This explanation is also consistent with the basic theory of the conservation of momentum where the area under the impact force versus time curve is equal to the total impulse acting on one body (say the missile) and also equal to the change in momentum. For these three cases, the change in momentum is the same, as the missile has the same mass and impact velocity. Therefore for the case of impact at Point C2, where the change in impulse occurs over a longer time, the peak force should be smaller than for the impact at Point A1, which agrees with the results.

6.2.5 Impact Testing – Plastic Cladding Response

After studying the elastic behaviour response of the cladding, a series of impact tests were conducted using both the 0.775 kg and 4 kg timber missiles to study the plastic cladding response. Target impact velocities were set in order to achieve certain impact conditions in terms of missile momentum and kinetic energy. The missile impact locations on the cladding specimen investigated were A1, B1 and C2. For this series of tests, only a single sheet of cladding was installed for simplified installation and handling. Justification for this modified set-up originated from the static deflection tests were it was proven that the force transfer across corrugations is negligible.

The following result, analysis and discussion consider only measured reaction forces in the z-direction, i.e. perpendicular to the cladding surface. The forces in this direction are much larger than the in-cladding plane forces and it is indeed these normal forces that induce damage and failure to the cladding material.

Detailed analysis was conducted for the impact scenarios where the momentum and/or kinetic energy were nominally the same for both missiles investigated. This allowed further insight into whether one of these factors had a predominant influence and, if so, which one.

The results of the impact tests are presented in Figure 26 in terms of the measured reaction force in the z-direction at A0 versus the missile momentum.

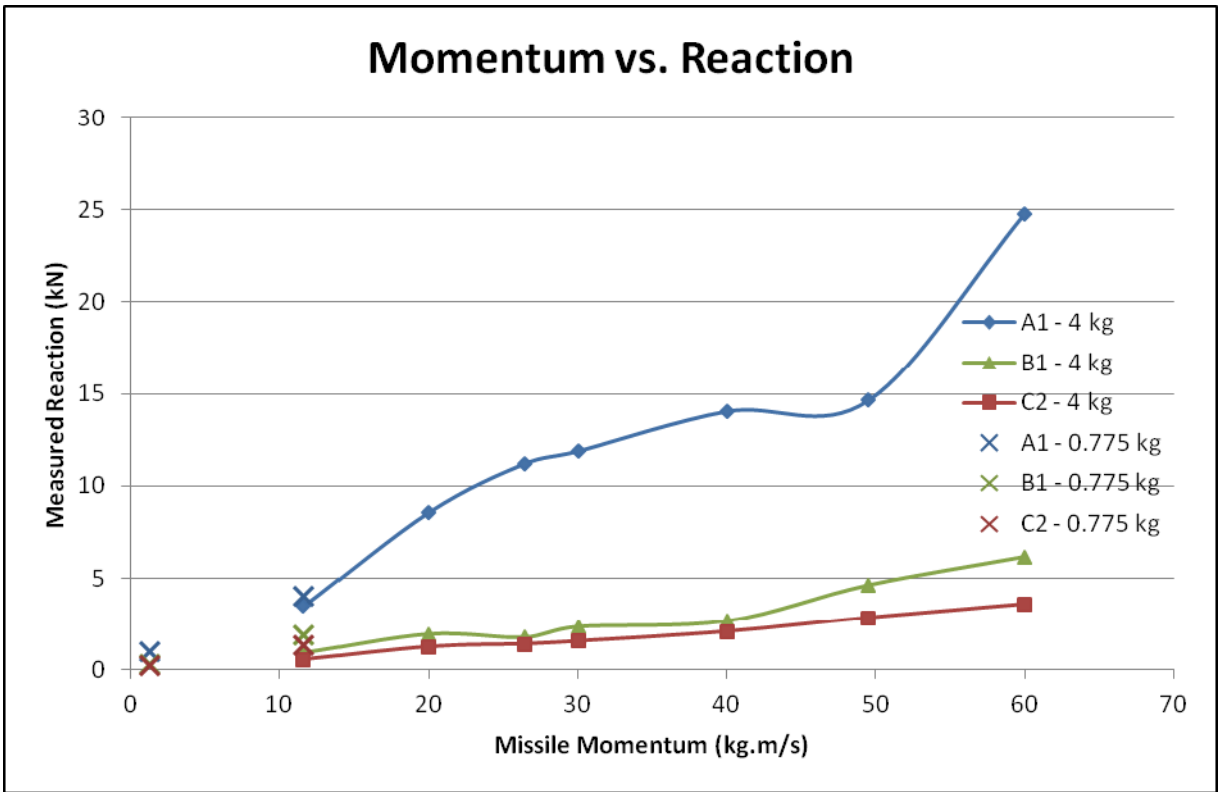

Figure 26: $R_{z,\,A0}$ vs. missile momentum for impacts at A1, B1 and C2

Comparing the recorded data for the two missiles with equal momentum, the plot shows that for impacts at location A1 the measured reaction appears to be closely related to the missile momentum, i.e. be a function of velocity only and independent of the missile mass. For impacts further away from the support and the girt to structure interface, the reactions

measured almost double for impacts with the smaller missile compared to the heavy missile with nominally equal momentum. The compared results and ratios of measured reaction forces are given in Table 3. The ratios are defined as $r = (R_{z,\ 0.775\ kg})/(R_{z,\ 4\ kg})$.

Table 3: Comparison of results for different missiles with equal momentum

Impact Location	Missile Mass (kg)	Missile Momentum (kg.m/s)	Max Measured z Reaction Force (kN)	Reaction Force Ratio
A1	0.775	11.6	4.06	1.16
	4		3.49	
B1	0.775		1.92	2.16
	4		0.89	
C2	0.775		1.36	2.57
	4		0.53	

Figure 27 is a plot of the measured results in terms of the measured reaction force in the z-direction at A0 versus the missile kinetic energy.

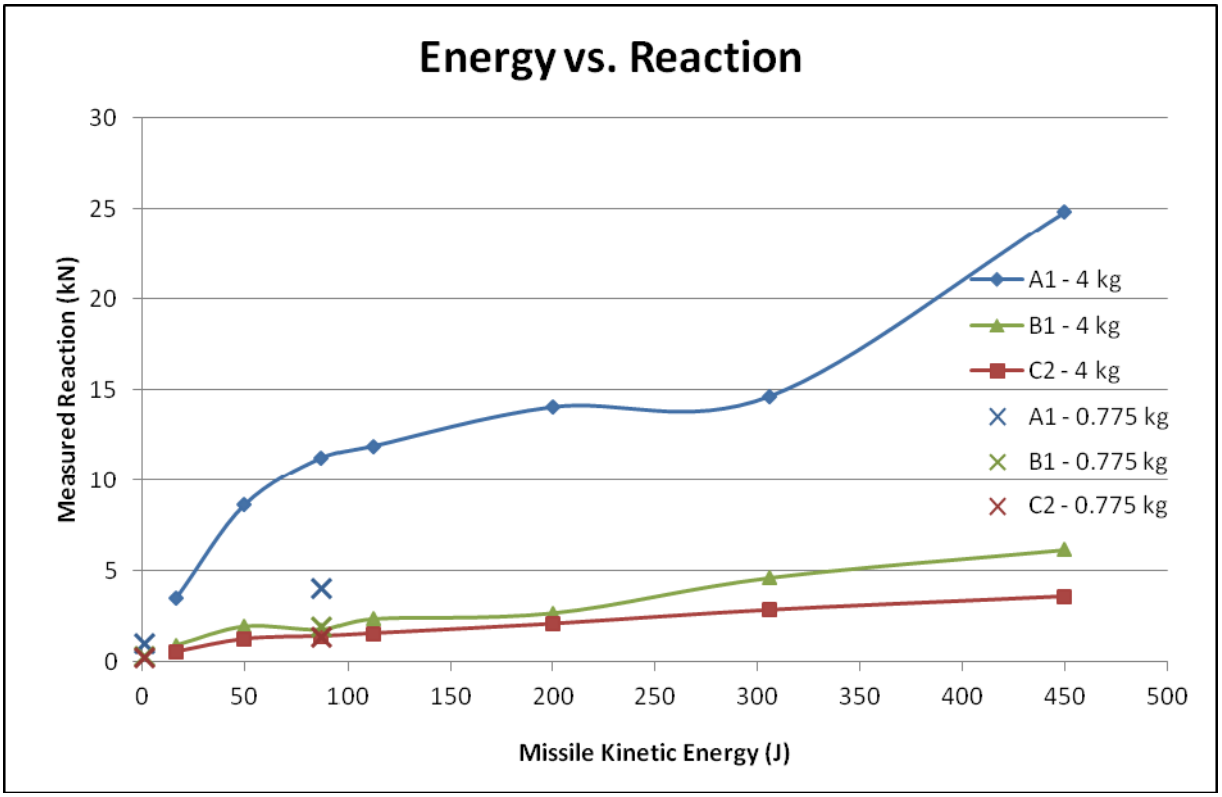

Figure 27: $R_{z,\ A0}$ vs. missile kinetic energy for impacts at A1, B1 and C2

In contrast to the plot in Figure 26, at impact locations B1 and C2 the measured reaction at A0 agrees very well for the two missiles at nominally equal kinetic energy. However, at impact location A1 the measured reaction is nearly three times larger for the larger missile carrying the same kinetic energy as the small missile; for this impact location there was good agreement when the missile momentum was considered. A comparison of results including reaction force ratios for impacts with different missiles at nominally equal kinetic energy is presented in Table 4.

Table 4: Comparison of results for different missiles with equal kinetic energy

Impact Location	Missile Mass (kg)	Missile Energy (J)	Max Measured z Reaction Force (kN)	Reaction Force Ratio
A1	0.775	87.2	4.06	0.36
	4		11.21	
B1	0.775		1.92	1.10
	4		1.75	
C2	0.775		1.36	0.98
	4		1.39	

The results indicate that the reaction force at the girt-structure interface is a quantitative representation of damage caused by impacting windborne debris. Accordingly, Tables 3 and 4 suggest that when the impact takes place on or near the girt, the damage caused can be directly related to the missile's momentum. When the impact occurs in the free spanning cladding region, the measured reaction force and hence the damage can be directly related to the missile's kinetic energy. Looking at the previously discussed qualitative test results (see Section 6.1.1) and the observations, these quantitative results confirm the hypothesis of energy absorption by cladding deformation.

From a practical point of view, windborne debris impacting directly on a support is not really a concern because these locations are not susceptible to failure in terms of debris penetrating. This statement will hold up to the point where a support member gets severely deformed and yields locally, leading to loss of structural stability and integrity. In this case, subsequent wind or debris loading may further damage the structural member or even dislodge attached cladding elements. For windborne debris to create a dominant opening in the building envelope or, in the more severe case, to pose a threat to occupant safety, the impact has to take place away from the support, i.e. in the free spanning region of the building envelope. Based on this reasoning, the governing parameter with regards to damage potential is the kinetic energy of the missile. But in reality the cladding's free spanning region starts only a few millimetres away from the support and intuitive judgment would suggest the response of the wall system (in terms of structural reaction) to be governed by a combination of both the missile momentum and kinetic energy.

The findings presented in this report are applicable only to the specific configuration investigated, i.e. 0.42 mm BMT corrugated G550 steel cladding in a single span set-up spanning 900 mm. It may be assumed that other cladding profiles made from the same material would behave and perform in a similar manner. However, this would need to be experimentally confirmed as would the cases of multi-span configurations and systems with different cladding span lengths. Following the hypothesis of energy absorption by plastic deformation, it seems logical that short internal spans of a multi-span system may be most prone to failure (by shear punch followed by rupture) due to increased stiffness and lack of flexibility allowing deformation.

7 CONCLUSIONS AND RECOMMENDATIONS

This report provides a comprehensive overview of the current state of knowledge of the field of windborne debris impact and cladding response. Topics discussed included the theory of object flight initiation due to wind forces, classification of debris types for use in theoretical analysis, their realistically attainable flight velocities and current applicable testing standards.

Based on observations after windstorm events and theoretical analyses, a range of debris types (shape, size, and mass) can be generated in windstorms and become missiles. The missiles can travel at a range of speeds, depending on the type, wind speed and also available space to allow acceleration. Eventually the missile will be stopped, possibly by impacting the envelope of a building. All building components that are susceptible to windborne debris impact, (i.e. the entire building envelope), have been described in detail.

The damage to the building envelope will depend on the missile (type), impact parameters (velocity, momentum and energy) and the characteristics of the envelope itself. A range of building envelope components and systems has been tested qualitatively to current standards to assess their resistance to windborne debris impact. General conclusions based on visual inspections of these qualitative impact tests were derived as follows:

- Failure mechanism is typically a shear punch
- Stiff systems/locations are more susceptible to this shear punch
- Energy absorption due to plastic deformation is beneficial
- Stiff, brittle materials cannot deform much and thus are prone to be penetrated by missiles

The quantitative response of a typical corrugated steel clad wall system was studied by measuring the reaction forces at a girt to structure interface when the cladding was subjected to static loading and a range of impact loads.

The largest shear force is experienced by the cladding when the load is applied adjacent to a support for both static and impact loading. With increasing distance away from the support, up to midspan, the load is shared by the other support. For the impact loading, the applied load also decreases more rapidly with increasing distance between the support and the point of load application due to deflection and elastic/plastic deformation of the cladding.

The impact loading generates large peak reaction forces at the girt to structure interface over very small time periods in the order of milliseconds. The magnitude of these forces and the time it takes between first contact of missile and cladding and arrival of the peak at the point of measurement depend on the location of impact which in turn relates to the difference in relative stiffness of the different target locations. This research suggests that if the missile impacts at a location with a relatively smaller stiffness (e.g. cladding well away from the supports), the cladding can deform more and so absorb energy over a longer time interval, with an associated reduction in the peak contact force between the missile and the target. The converse is true for impacts where the target stiffness is relatively larger, that is a shorter time period to reach a larger force. This explanation is also consistent with the basic theory of the conservation of momentum where the area under the impact force versus time curve is equal to the total impulse acting on the missile and also equal to the change in momentum

The magnitudes of the reaction forces are related to the momentum and kinetic energy of the impacting missile and depend on the elastic/plastic response of the cladding, which in turn is dependent on the impact location. Energy absorption by the cladding is much more pronounced when the missile impact is close to the cladding midspan; in this region the cladding is able to deflect and plastically deform more which is the prime mechanism of energy absorption. In this cladding region, the measured reaction forces relate closely to a given missile's kinetic energy, independent of the missile's mass or impact velocity. For impacts close to the support (and hence the girt to structure interface), the cladding is restrained from deflecting and deforming plastically due to the introduced stiffness of its connection to the support. In this cladding area, the measured reaction forces are closely related to the impacting missile's momentum, regardless of its mass and impact velocity.

8 REFERENCES

Concrete Masonry Association of Australia. (2007). Concrete Masonry Handbook.

Ginger, J., Leitch, C., Henderson, D., & Reitano, C. (2004). *Flying Debris Impact in Windstorms.* Paper presented at the International Conference on Building Envelope Systems and Techonologies, Sydney.

Holmes, J. D. (2007). *Wind loading of structures* (2 ed.): Taylor & Francis Group.

Leitch, C., Ginger, J., Harper, B., Kim, P., Jayasinghe, N., & Somerville, L. (2009). Investigation of Performance of Housing in Brisbane Following Storms on 16 and 19 November 2008 *Technical Report (James Cook University, Cyclone Testing Station)*. Townsville.

Lin, N., Holmes, J. D., & Letchford, C. W. (2007). Trajectories of wind-borne debris in horizontal winds and applications to impact testing. *Journal of Structural Engineering-Asce, 133*(2), 274-282.

Queensland Government, Department of Public Works. (2006). Design Guidelines for Queensland Public Cyclone Shelters

Reitano, C. (2003). *Flying Debris Damage Potential in Windstorms.* Bachelor of ENgineering, James Cook University, Townsville.

Richards, P., Pe, K., & Milne, I. (2009). *Impact Dynamics of Rod Type Windborne Debris.* Paper presented at the Seventh Asia-pacific Conference on Wind Engineering, Taipei.

Rogers, Colin A., & Hancock, Gregory J. (1997). Ductility of G550 Sheet Steels in Tension. *Journal of Structural Engineering, 123*(12), 1586-1594.

Standards Australia. (2011). AS/NZS1170.2: Structural design actions - Wind actions.

Wills, J. A. B., Lee, B. E., & Wyatt, T. A. (2002). A model of wind-borne debris damage. *Journal of Wind Engineering and Industrial Aerodynamics, 90*(4-5), 555-565.

Wills, J. A. B., Wyatt, T. A., & Lee, B. E. (1998). Warnings of high winds in densely populated areas *IDNDR Flagship Programme*. London.